Article

Not peer-reviewed version

Dirac Fermion of a Monopole Pair (MP) Model

Samuel Yuguru *

Posted Date: 22 August 2024

doi: 10.20944/preprints202210.0172.v12

Keywords: Dirac fermion; Quantum field theory; Dirac belt-trick; space-time; quantum mechanics; Lie group; Dirac field theory

 doi:10.20944/preprints202210.0172.v12

Article

Dirac Fermion of a Monopole Pair (MP) Model

Samuel. P. Yuguru

Department of Chemistry, School of Natural and Physical Sciences, University of Papua New Guinea, P. O. Box 320, Waigani Campus, National Capital District 134, Papua New Guinea, Tel. : +675 326 7102; Fax. : +675 326 0369; Email address: samuel.yuguru@upng.ac.pg.

Abstract: The electron of spin −1/2 is a Dirac fermion of a complex four-component spinor field. Though it is effectively addressed by relativistic quantum field theory (QFT), an intuitive form of the fermion still remains lacking and it is often speculated by Dirac belt trick or its related analogies. In a similar fashion, the interpretation of Dirac fermion by QFT is examined within a recently proposed MP model of a hydrogen atom into 4D space-time. The model consists of clockwise precession of an elliptical MP field mimicking Dirac string and an electron of physical entity in orbit of time reversal. Such dynamics sustains charge conjugate, parity inversion and time reversal symmetry with the transition of the electron to Dirac fermion being consistent with Dirac belt trick, quantum mechanics and Lie group. The electron path is solenoidal to on-shell momentum of circular Bohr obit (BO), and by disturbance, this levitates and dissects the MP field of electric dipole moment into n-dimensions of Minkowski space-time. Contraction of BOs towards the vertices generates instanton magnetic monopoles into Euclidean space-time by clockwise precession of the MP field to induce a spherical model. These outcomes are compatible with Dirac field theory and its related components like wave function collapse, quantized Hamiltonian, non-relativistic wave function, Weyl spinor, Lorentz transformation and electroweak symmetry breaking mechanism. The model though speculative, its dynamics can become important towards defining the fundamental state of matter as demonstrated in this study and this warrants further investigations.

Keywords: dirac fermion; quantum field theory; dirac belt-trick; space-time; quantum mechanics; lie group; dirac field theory

1. Introduction

At the fundamental level of matter, particles are described by wave-particle duality, charges and their spin property. These properties are revealed from light interactions and are pursued by the application of relativistic QFT [1,2]. The theory of special relativity defines lightspeed, c to be constant in a vacuum and its particle-like property consist of massless photon of spin 1 with a neutral charge. Any differences to photon's spin, charge and mass-energy equivalence by, $m = E/c^2$ provide the inherent properties of matter particles such as fermions of spin ±1/2 and this is termed causality [3,4]. Based on QFT, particles appear as excitation of fields permeating space at less than lightspeed. Within the atom, the electron is a fermion and its position is defined by non-relativistic Schrödinger's wave function, ψ of probabilistic distribution [5]. A level of indetermination is associated with the observation of its spin-charge property, whereas the wave-particle duality is depended on the instrumental set-up [6,7]. Based on quantum mechanics interpretation, the atom radiates energy in quantized form, nhv of infinitesimal steps. When this is incorporated into QFT, it becomes difficult to imagine wavy form of particles such as electrons freely permeating space without interactions and this somehow collapses to a point at observation [8]. Similarly, the resistive nature of proton decay [9] somehow suggests the preservation of the electron and hence, atom to balance out the charges. While proton decay is an active topic of research, in the meantime, the preferred quest is to make non-relativistic equations become relativistic due to the shared properties of both matter and light at the fundamental level as mentioned above.

Beginning with Klein-Gordon equation [10], the energy and momentum operators of Schrödinger equation,

 doi:10.20944/preprints202210.0172.v12

$$\hat{E} = i\hbar\frac{\partial}{\partial t}, \qquad \hat{p} = -i\hbar\boldsymbol{\nabla}, \tag{1}$$

are adapted in the expression,

$$\left(\hbar^2\frac{\partial^2}{\partial t^2} - c^2\hbar^2\boldsymbol{\nabla}^2 + m^2c^4\right)\psi(t,\bar{x}) = 0. \tag{2}$$

Equation (2) incorporates special relativity, $E^2 = p^2c^2 + m^2c^4$ for mass-energy equivalence, $\boldsymbol{\nabla}$ is the del operator in 3D space, $\hbar$ is reduced Planck constant and i is an imaginary number, $i = \sqrt{-1}$. Only one component is considered in Equation (2) and it does not take into account the negative energy contribution from antimatter. In contrast, the Hamiltonian operator, $\hat{H}$ of Dirac equation [11] for a free particle is,

$$\hat{H}\psi = (-i\boldsymbol{\nabla}.\boldsymbol{\alpha} + m\beta)\psi. \tag{3}$$

The ψ has four-components of fields, i with vectors of momentum,∇ and gamma matrices, α, β represent Pauli matrices and unitarity. The concept is akin to, $e^+ e^- \longrightarrow 2\gamma$, where the electron annihilates with its antimatter to produce two gamma rays. Antimatter existence is readily observed in both Stern-Gerlach experiment and positron from cosmic rays. The relationship between matter and antimatter at the subatomic level is described by charge conjugation (C), parity inversion (P) and time reversal (T) symmetry. Charge conjugation reverses the charge without changing the direction of the spin vector or momentum of the particle. Only time reversal accounts for changes in the spin direction. Parity is discreet space-time symmetry offered by spatial coordinates and these are invariant under inversion when the charge is reversed. Based on QFT, numerous literatures explore these parameters in order to explain the anomaly of the dominance of matter over antimatter and space-time quantization. The electron dominance over its conjugate pair is explained by 360° rotation, where a positron is generated. Another 360° rotation for a total of 720° rotation and the electron is restored to its original state. The process offers the helical property of the electron as a fermion of fractional spin and is described by so-called Dirac belt trick [13] in an attempt to capture the CPT symmetry. Other related descriptions include Balinese cup trick [14] or Dirac scissors problem [15]. The notion of space-time at singularity, where the electron translates to positron and vice versa is not well defined with respect to CPT symmetry. One way to visualize space-time in 4D is from Klein bottle topology of 2D manifold [16], where spin vector varies within the manifold without a reference point-boundary akin to a sphere. Quantum gravity at singularity is analogous to discrete space-time on geometry basis, where CPT symmetry becomes prominent for particles assuming its own antimatter like the electron. Quantum gravity or quantized state of gravitational field requires the existence of graviton, a spin 2 particle and this is yet to be positively identified in both high energy physics experiments and gravitational waves emanating from astronomical sources.

In this study, how Dirac fermion is interpretable within a MP model mimicking hydrogen atom of 4D space-time is examined. The orbit of the electron of a charged particle is of time reversal imposed on a clockwise precession of elliptical MP field mimicking Dirac string. These connotations of matter and space-time dynamics can accommodate both CPT symmetry and the transformation of the electron into a Dirac fermion of a complex spinor by Dirac belt trick. This appears consistent with quantum mechanics and Lie group on geometry basis. The electron orbit of solenoidal into n-dimensions of both Minkowski and Euclidean space-times is relevant to the emergence of monopole at the vertex of the MP field of electric dipole moment. These outcomes are compatible with Dirac field theory and its associated components like wave function collapse, quantized Hamiltonian, non-relativistic wave function, Weyl spinor, Lorentz transformation and electroweak symmetry breaking mechanism. Though the model remains a speculative tool, it can become important towards defining the fundamental state of matter as shown in this study and this requires further examinations by conventional methods.

 doi:10.20944/preprints202210.0172.v12

2. An Electron Conversion to a Fermion by Dirac Process

In this section, the transformation of an electron of hydrogen atom type of 4D space to a fermion by Dirac process is examined within a spherical MP model (Figure 1a–d). First the process of Dirac belt trick is demonstrated for the electron-positron transition process. Second, the relevance of the model to basic interpretations of quantum mechanics, Lie Group, center of mass (COM) reference frame and its dynamics are described before pursuing its implications to QFT.

2.1. Unveiling Dirac Belt Trick within the Spherical MP Model

The electron orbit of time reversal in discrete continuum form of sinusoidal wave is defined by Planck radiation, h. In forward time, the orbit is transformed into an elliptical shape of a MP pair field somewhat mimicking Dirac string (Figure 1a). With clockwise precession, the torque or right-handedness exerted on the MP field shifts the electron of spin up from positions 0 to 4 to assume 360° rotation. Time reversal orbit against clockwise precession allows for maximum twist at the point-boundary or vertex of the MP field at position 4. The electron then flips to spin down mimicking a positron to begin the unfolding process and emits radiation by, $E = nhv$. The positron is short-lived from possible repulsion of the proton and by another 360° rotation from positions 5 to 8, the electron is restored to its original state. The electron-positron transition is attained within a hemisphere of the MP field that is interchangeable with the other hemisphere and this sustains CPT symmetry. These intuitions are analogous to Dirac belt trick at 720° rotation with positions 0 to 3 and its transposition at positions 4 to 8 assigned to Dirac four-component spinor, $\psi = \begin{pmatrix} \psi_0 \\ \psi_1 \\ \psi_2 \\ \psi_3 \end{pmatrix}$ at spherical lightspeed. The conjugate pairs of positions, 1, 3 and 5,7 cancels out the charges to form loops of Bohr orbits (BOs). These levitates into n-dimensions of energy levels by disturbance to generate Minkowski space-time (Figure 1b). The emergence of light-cones depict Weyl spinor and singularity at the center is restricted from external observations by the electron's shift at positions 2 and 6 and this is explored later in section 2d. Additional details on the conceptualization path of the model from electron wave-diffraction is offered elsewhere [17]. Clockwise precession by spherical lightspeed presents an inertia reference frame, λ (Figure 1a) under the conditions,

$$\lambda_{\pm}^2 = \lambda_{\pm} \quad Tr\lambda_{\pm} = 2\,\lambda_{+} + \lambda_{-} = 1, \tag{4}$$

where the trace function, Tr is the sum of all elements within the model. These elements are pertinent to quantum mechanics, QFT and the Lie group as presented next.

Preprints.org (www.preprints.org) | NOT PEER-REVIEWED | Posted: 22 August 2024 doi:10.20944/preprints202210.0172.v12

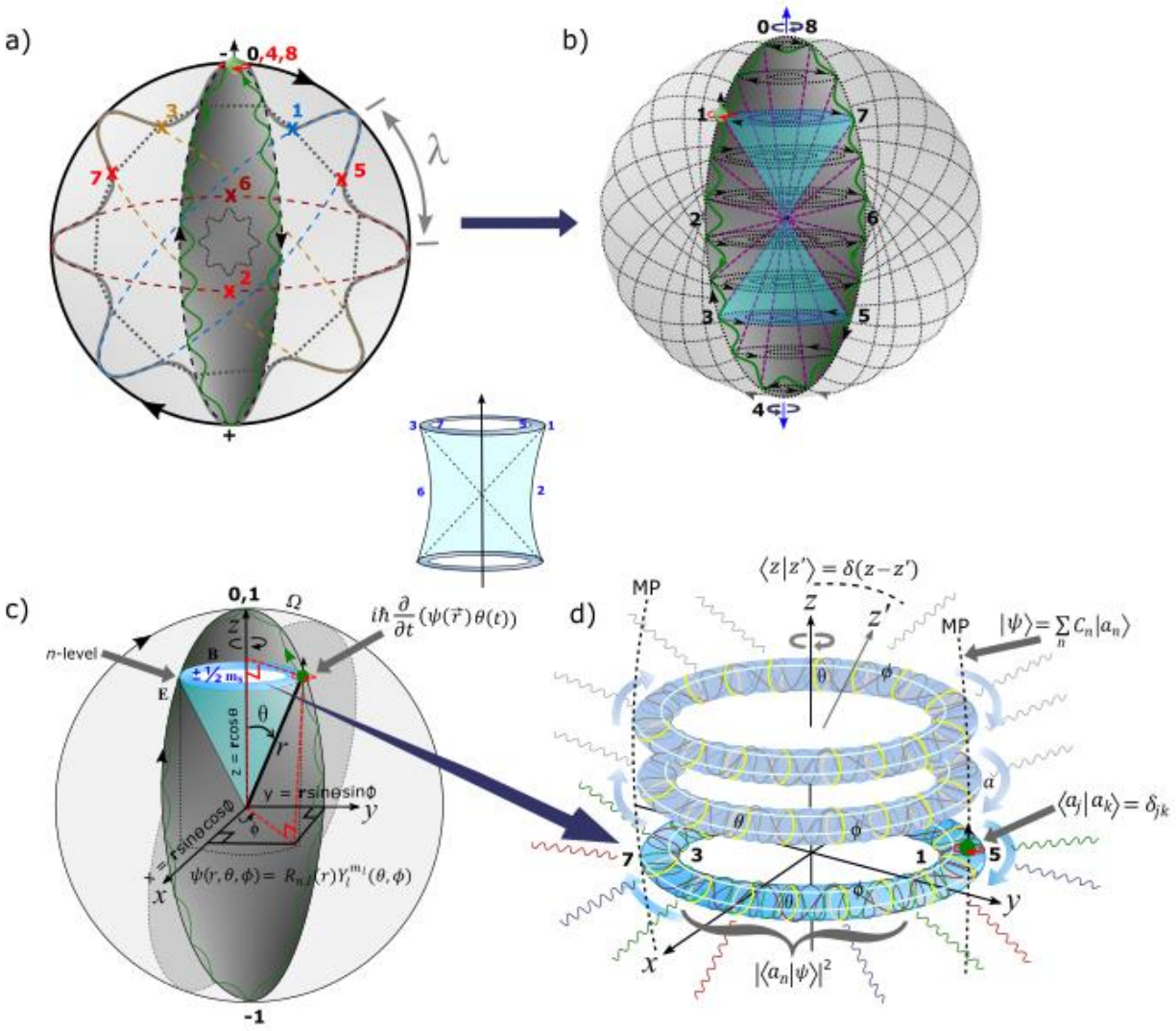

Figure 1. The MP model [17]. (a) In flat space, a spinning electron (green dot) in orbit of sinusoidal form (green curve) is of time reversal. It is normalized to an elliptical MP field (black area) of a magnetic field, **B** mimicking Dirac string. By clockwise precession (black arrows), an electric field, **E** of inertia frame, λ is generated. The shift in the electron's position from positions 0 to 4 at 360° rotation against clockwise precession offers maximum twist. At position 4, the electron flips to a positron to begin the unfolding process from positions 5 to 8 for another 360° rotation to restore the electron to its original state analogous to Dirac belt trick. For the total of 720° rotation, a dipole moment (±) is generated for the spherical model with CPT symmetry sustained for the electron. (b) The BOs are defined by conjugate numbered pairs, 1,3 and 5,7, where cancellation of charges allows for the emergence of angular momentum (purple dotted lines) of spin ±1/2 (navy colored light-cones) with vectors aligned to the vertices of the MP field at positions 0 and 4. Levitation of BOs into n-dimensions of Minkowski space-time is by disturbance. These are projected in degeneracy towards the center and by contraction to the vertices of the spherical model as Euclidean space-time. (c) The electron in orbit is tangential to smooth manifold of BO intersecting the MP field and this is relevant to Lie group. With precession stages, Ω, at spherical lightspeed the model is polarized to qubits, 0 and ±1 at the vertices of the MP field for classical computing. The polar coordinates (r, θ, Φ) are attributed to Schrödinger wave function with respect to the electron's position in space. (d) Topological torus emerges from BO defined by ϕ (white loops) and its dissection perpendicularly by θ (yellow circles) from intermittent clockwise precession stages of the MP field. Any light-matter interactions are tangential to the electron's position at the base point of BOs. Levitation of manifolds of BOs into n-dimensions of Minkowski space-time is solenoidal by linearization along the principle axis of the MP field as time axis in asymmetry. Singularity at the center for the light-cone is constrained by electron's

 doi:10.20944/preprints202210.0172.v12

shift at positions, 2 and 6 along horizontal *x*-*y* plane of an irreducible spinor field (insert centered image). The embedded terms and equations are explained in the text

2.2. *Quantum mechanics and Dirac notations*

The transformation of the electron to a Dirac fermion can accommodate some basic concepts in quantum mechanics and QFT (Figure 1c,d). These are outlined below in bullet points based on ref. [18].

- The electron of wave-particle duality obeys de Broglie relationship, $\lambda = h/mv$ with h assigned to its sinusoidal orbit and mv to BO. It is defined by the wave function, ψ and its orbit of time reversal adheres to the Schrödinger equation, $i\hbar\frac{\partial}{\partial t}(\psi(\vec{r})\theta(t))$ in space-time (Figure 1c) (see also Appendix A for further explanations). Its superposition state (electron-positron pair) in space is linked to BO defined by ϕ and thus, its inner product is, $\langle\psi|\phi\rangle^* = \langle\psi|\phi\rangle$ with respect to *z*-axis. Conjugate charges at positions, 1, 3 and 5 and 7 cancels each other out at spherical lightspeed to form close loops, where the electron is stabilized to generate only either spin up or spin down in its orbit at an energy *n*-level in accordance with Pauli exclusion principle. At 360° rotation, an electron of spin up is produced and at 720° rotation, a positron of spin down is formed. The loops of BOs are topology construct of differential manifolds into *n*-levels or *n*-dimensions by levitation due to disturbance (Figure 1d). In this way, the electron forms a weak isospin, whereas the *z*-axis mimicking spin up and spin down resembles nuclear isospin.
- Both radial and angular wave functions are applicable to the electron, $\psi(r,\theta,\phi) = R_{n,l}(r)Y_l^{m_l}(\theta,\phi)$. The radial part, $R_{n,l}$ is attributed to the principal quantum number, n and angular momentum, l of a light-cone with respect to r (Figure 1c). The angular part, $Y_l^{m_l}$ in degenerate states, $\pm m_l$ with respect to the *z*-axis is assigned to the BO defined by both θ and ϕ (Figure 1d).
- The BO is defined by a constant structure, a and its orthogonal (perpendicular) to *z*-axis by linearization (Figure 1d). Its link to electron-positron pair is, $\langle a_j|a_k\rangle = \int dx\psi_{a_j}^*(x)\psi_{a_k}(x) = \delta_{jk}$ for continuous derivation by rotation and is relevant to Fourier transform (see also Appendix B). Linear translation for the *n*-levels along *z*-axis can relate to the sum of expansion coefficients, C_n, where the electron's position offers an expectant value, $|\psi\rangle = \sum_n C_n/a_n\rangle$. Its probability is of the type, $\langle a_n|\psi\rangle^2$.
- The shift in the electron's position of hermitian conjugates by Dirac process, $P(0\rightarrow 8) = \int_\tau^{\square}\psi^*\hat{H}\psi d\tau$ assumes Hamiltonian space with τ by precession (Appendix B). The complete spherical rotation towards the point-boundary for the polarization states, 0, 1 assumes U(1) symmetry and incorporates Euler's formula, $e^{i\pi} + 1 = 0$ in real space for classical computing (Figure 1c).
- Singularity at Planck's length is assigned to the point-boundary at position 0 and this promotes radiation of the type, $E = nhv$ by the electron-positron transition. Somehow it sustains the principle axis of the MP field as *z*-axis or nuclear isospin in asymmetry and this sustains ±h at spherical lightspeed.

2.3. *Lie Group*

The geometry of the MP model is relevant to Lie group of differential smooth manifolds and this is attributed to both BO of a circle and the spherical model (Figure 1c). The BO in degeneracy is topological into *n*-dimensions by levitation due to disturbance. Electron-light interaction appears tangential to the manifolds of BOs of non-abelian and this generates a solenoid with $\nabla.B = \mu_0\rho$ (Figure 1d). At the vertices of the MP field at positions 0 and 4 (Figure 1c), the solenoid of *n*-dimensions of BOs by levitation (Figure 1d) is reduced to singularity with $\nabla.B = 0$ and the electron is transformed to a monopole. The monopole is not transferrable by linearization possibly due to coupling of the vertices of the MP field of Dirac string somewhat mimicking a little magnet. Moreover, the electron transition polarizes the MP field to generate an electric dipole moment of quantized electric charge such as $\nabla.E = \rho/\varepsilon_0$.

 doi:10.20944/preprints202210.0172.v12

Rotation matrices of the type, $Rr_{yz}(\theta)$ and $R_{zx}(\theta)$ is attributed to the MP field by precession with any shift in z-axis of nuclear isospin trivial, $\langle z|z'\rangle = \delta(z - z')$ (Figure 1d). The rotation matrix, $R_{xy}(\theta)$ is assigned to the BO into n-dimensions. These are relevant to describe both integer and half-integer spins such as, 0, 1/2 and 1 towards complete rotation at position 0 at the point-boundary. These attributes are presented in Figure 2A of Appendix B with some examples are explored in here based on refs. [19,20].

Chirality of the electron is described by,

$$g \in G, \tag{5}$$

where g is the electron's position as subset of the space tangential to the manifolds and G represents the Lie group. For the conjugate numbered pairs, 1, 3 and 5, 7 of BO (Figure 1d), Equation (5) validates the operations,

$$g_{1,5} + g_{3,7} \in G \tag{6a}$$

and

$$g + (-g) = i, \tag{6b}$$

where i is spin matrix for both spin ±1/2 (Figure 2A). The form, $g_1 + g_3 \neq g_5 + g_7$ due to electron-positron ($\pm g$) transition and radiation loss, $E = nhv$ tangential to the manifolds. For linear transformation along z-axis in 1D space, the BOs are isomorphic with respect to the particle position, $|\psi\rangle = \sum_n C_n/a_n\rangle$ (Figure 1d and 2A). By intermittent precession, the inner product of r is a scalar and relates to the boundary of the MP field in the form,

$$\vec{r}_1 \,.\, \vec{r}_2 = |\vec{r}_1 \,||\, \vec{r}_2| cos\theta \tag{7}$$

where rotation of both vectors preserve the lengths and relative angles (e.g., Figure 1c). By assigning rotation matrix, R to Equation (7), its transposition is,

$$(Rr_1)^T(Rr_2) = r_1^T r_2 I, \tag{8}$$

where the identity matrix, $I = R^T \times R$ by reduction (Figure 2A). The orthogonal relationship of BO to clockwise precession along z-axis at 90° for all rotations suggests, $R \in$ SO(3). The SO(3) group rotation for integer spin 1 in 3D space is,

$$R_{yz}(\theta) = \begin{pmatrix} 1 & 0 & 0 \\ 0 & cos\theta & -sin\theta \\ 0 & sin\theta & cos\theta \end{pmatrix} \begin{pmatrix} x \\ y \\ z \end{pmatrix}. \tag{9}$$

Equation (9) can also be pursued for integer spin 0 and higher spin particles. When rotating as 2 x 2 Pauli vector for SU(2) symmetry with respect to a light-cone of half-integer spin (Figure 1d), Equation (9) translates to the form,

$$\pm \begin{pmatrix} cos\frac{\theta}{2} & isin\frac{\theta}{2} \\ isin\frac{\theta}{2} & cos\frac{\theta}{2} \end{pmatrix} = \begin{pmatrix} z & x - y_i \\ x + y_i & -z \end{pmatrix} = \begin{vmatrix} \xi_1 \\ \xi_2 \end{vmatrix} |-\xi_2 \quad \xi_1|, \tag{10}$$

where ξ_1 and ξ_2 are Pauli spinors of rank 1 to rank 1/2 tensor relevant for Dirac matrices (Figure 2A). By orthogonal geometry, the column is attributed θ at n-levels along z-axis and the row to BO defined by ϕ in degeneracy. For ladder operators at n-dimension along z-axis, SU(2) is irreducible for the shift in θ and ϕ such as, $\binom{SU(2)}{n \times n} \neq \binom{SU(2)}{l \times l} \oplus \binom{SU(2)}{m \times m}$. Translation of SU(2) by accentuating precession at high energy like, $\binom{SU(2)}{2 \times 2} \oplus \binom{SU(2)}{2 \times 2}$ matrices is reduced to the upright MP field position (e.g., Figure 1b). For the particle's position, when $y = 0$, $z = x$ is a real number. At $x = 0$, $z = y$ becomes an imaginary number. The BO linked to the electron's position can be assigned to SO(2) group in 2D such as,

 doi:10.20944/preprints202210.0172.v12

$$\begin{pmatrix} cos\theta & sin\theta \\ -sin\theta & cos\theta \end{pmatrix} \cong \begin{pmatrix} 1 & \theta \\ -\theta & 1 \end{pmatrix} = I + \theta \begin{pmatrix} 0 & 1 \\ -1 & 0 \end{pmatrix}, \quad (11)$$

where, $\theta \in [0,2\pi]$ incorporates Dirac process at 720° rotation (e.g., Figure 1a). Similar relationships can be forged for $R_{xy}(\phi)$ with respect to the BO along x-y plane with respect to Equation (9) in the form,

$$R_{xy}(\phi) = \begin{pmatrix} cos\phi & -sin\phi & 0 \\ sin\phi & cos\phi & 0 \\ 0 & 0 & 1 \end{pmatrix} \begin{pmatrix} x \\ y \\ z \end{pmatrix} = \pm \begin{pmatrix} e^{i\frac{\phi}{2}} & 0 \\ 0 & e^{-i\frac{\phi}{2}} \end{pmatrix}. \quad (12)$$

Substitution of Equation (12) with $R_{xy}(\phi) = e^{\theta}$ can relate to polarization states, -1, 1 and 0 at the vertices of the MP field (Figure 1c) from the electron-positron transition such as,

$$e^{\theta} \begin{bmatrix} 0 & -1 & 0 \\ 1 & 0 & 0 \\ 0 & 0 & 0 \end{bmatrix} = \begin{bmatrix} cos\theta & -sin\theta & 0 \\ sin\theta & cos\theta & 0 \\ 0 & 0 & 1 \end{bmatrix}. \quad (13)$$

The matrices described by Equation (13) is relevant to Figure 2A. These explanations offer the basics to the complexities of compact Lie group similar to those demonstrated for quantum mechanics and Dirac notations in the preceding subsection.

2.4. Center of Mass Reference Frame and Its Dynamics

The center of mass (COM) is assigned to position 0 at the point-boundary or vertex of the elliptical MP field and is attributed to electron-positron transition. Some of its dynamics are described here. First, the COM is analogous to zero-point energy (ZPE) of the hydrogen atom of ultraviolet range of a harmonic oscillator. The oscillator can translate to a hemisphere of the MP field of Dirac string of time invariant and this can be stretched out towards COM of ZPE with its baseline assumed at positions 2 and 6 of superposition states from the electron-positron transition. Second, the electron's position in orbit is quantized into BOs of n-dimensions and this levitates by stretching into Minkowski space-time (Figure 1b). In this case, the COM is compared to instanton magnetic monopoles by precession of the MP field into Euclidean space-time. This is generated from reduction of the topology of solenoid of n-dimensions towards the spherical boundary (Figure 1d). Third, the COM of ZPE generates instantons from electron-positron transition as a consequence of twisting and unfolding by Dirac process. This is accessible to quantum tunneling with precession of the MP field at spherical lightspeed. Fourth, envelop solitons are applicable to positions 2 and 6 of the electron orbit at the baseline of the pair of hemispheres of the MP field. Stochastic behavior at these positions by electron-positron transition forms a chaotic atomic system of the hydrogen atom. Fifth, these positions offer fundamental graininess to classical limit of quantum mechanics by correspondence principle. The inertia frame, λ (Equation (4)) is transformed to relativistic Campton's atomic wavelength, $\lambda = h/mc$ for the MP model of hydrogen atom. Dissection of λ into n-dimensions of BOs as n-energy levels is analogous to both the line spectrum and vibrational spectrum of ionized hydrogen molecule. The envelop solitons then form rotational energy levels to the n-levels. Sixth, signals from the solitons of chaotic system either from electron-positron transition or its particle-hole symmetry by ejection of the electron is expected to conceal the point of singularity of the pair of light-cones (Figure 1b). This is relevant to high energy physics when infinite n-dimensions are set to one dimension linearly with natural units as $\varepsilon_0 = c = \hbar = 1$. By conservation, the particle-hole at positions 2 and 6 by coupling of ionized MP models can restrict direct observations of quarks and in turn generate asymptotic freedom. Conversely, where the chaotic system converges with the quantum critical region provided by the light-cones towards the baseline of the hemisphere (e.g., Figure 1a), this becomes important to the pursuit of quantum critical point such as in condensed matter physics for an array of atoms in one-dimensional line. Seventh, qubits 0, 1 and hypercharge –1 are assumed respectively at positions 0, 8 and 4 (Figure 1a,c). These are relevant to classical computing, whereas for quantum computing, the accessibility to the nucleons mimicking the MP model is restricted by the envelop solitons of the chaotic system at positions 2 and 6. Eight, COM is

 doi:10.20944/preprints202210.0172.v12

relevant to Coulomb's law of electric force, $F = \frac{1}{4\pi\varepsilon_0}.\frac{q_1.q_2}{r^2}$ between two charged bodies if these equate to electron-positron pair in a vacuum. The radius, *r* is assigned to the principle axis of the MP field (Figure 1a) and it links COM with the nucleus akin to nuclear isospin. The inertia frame of the model by precession at a constant velocity accommodates centripetal force. Finally, the electron of subatomic particle upholds the uncertainty principle of undefined position and momentum during its transition in orbit, whereas its relativistic analog of energy and time is applicable to linear light paths tangential to the spherical MP model. Similarly, Campton's wavelength defines the atomic MP model at spherical lightspeed.

3. Dirac Field Theory and Its Related Components

Further exposition of the helical property of the MP model to induce Dirac belt-trick is offered in Figure 2a–f. The CPT symmetry is sustained for the electron-positron transition at the point-boundary, where COM is assumed. The electron's time reversal orbit of a MP field mimics Dirac string and it is subjected to both twisting and unfolding process by clockwise precession. Cancellation of charges at conjugate positions 1, 3 and 5, 7 allows for the emergence of BO to accommodate either spin up or spin down states. The BOs of manifolds into *n*-dimensions by levitation are relevant to disturbance of the model (e.g., Figure 1d). How all these become compatible with the basics of Dirac theory and its associated components [1,2,10,11] are succinctly described here in bullet points in order to plot the path for further undertakings.

⇒ **Dirac theory and helical property.** The fermion field is defined by the famous Dirac equation of the generic form,

$$i\hbar\gamma^u\partial_u\psi(x) - mc\psi(x) = 0, \tag{14}$$

where γ^u are gamma matrices. The exponentials of the matrices, $\{\gamma^o\gamma^1\gamma^2\gamma^3\}$ are attributed to the electron's position by clockwise precession acting on its time reversal orbit. For example, $\gamma^o$is assigned to the vertex of the MP field and by electron-positron transition at position 0, it sustains *z*-axis as arrow of time in asymmetry. Thus, arrow of time for a pair of vertices for spin up and spin down incorporates time reversal symmetry. The $\gamma^1\gamma^2\gamma^3$ variables of Dirac matrices are assumed by the electron shift in its positions (Figure 2a–f). Orthogonal projections of the space-time variables, $\frac{1}{2}(1 \pm i\gamma^0\gamma^1\gamma^2\gamma^3)$ are confined to a hemisphere and assigned to a light-cone to generate spin-charge of the electron (e.g., Figure 1c). These descriptions uphold CPT symmetry and are indirectly incorporated into the famous Dirac equation,

$$\left(i\gamma^0\frac{\partial}{\partial t} + cA\frac{\partial}{\partial x} + cB\frac{\partial}{\partial y} + cC\frac{\partial}{\partial z} - \frac{mc^2}{\hbar}\right)\psi(t,\vec{x}), \tag{15}$$

where *c* acts on the coefficients A, B and C and transforms them to γ^1, γ^2 and γ^3. The exponentials of γ are denoted *i* for off-diagonal Pauli matrices for the light-cone (Figure 1d) and is defined by,

$$\gamma^i = \begin{pmatrix} 0 & \sigma^i \\ -\sigma^i & 0 \end{pmatrix}, \tag{16a}$$

and zero exponential, γ^o is,

$$\gamma^0 = \begin{pmatrix} 0 & 1 \\ 1 & 0 \end{pmatrix}. \tag{16b}$$

Preprints.org (www.preprints.org) | NOT PEER-REVIEWED | Posted: 22 August 2024 doi:10.20944/preprints202210.0172.v12

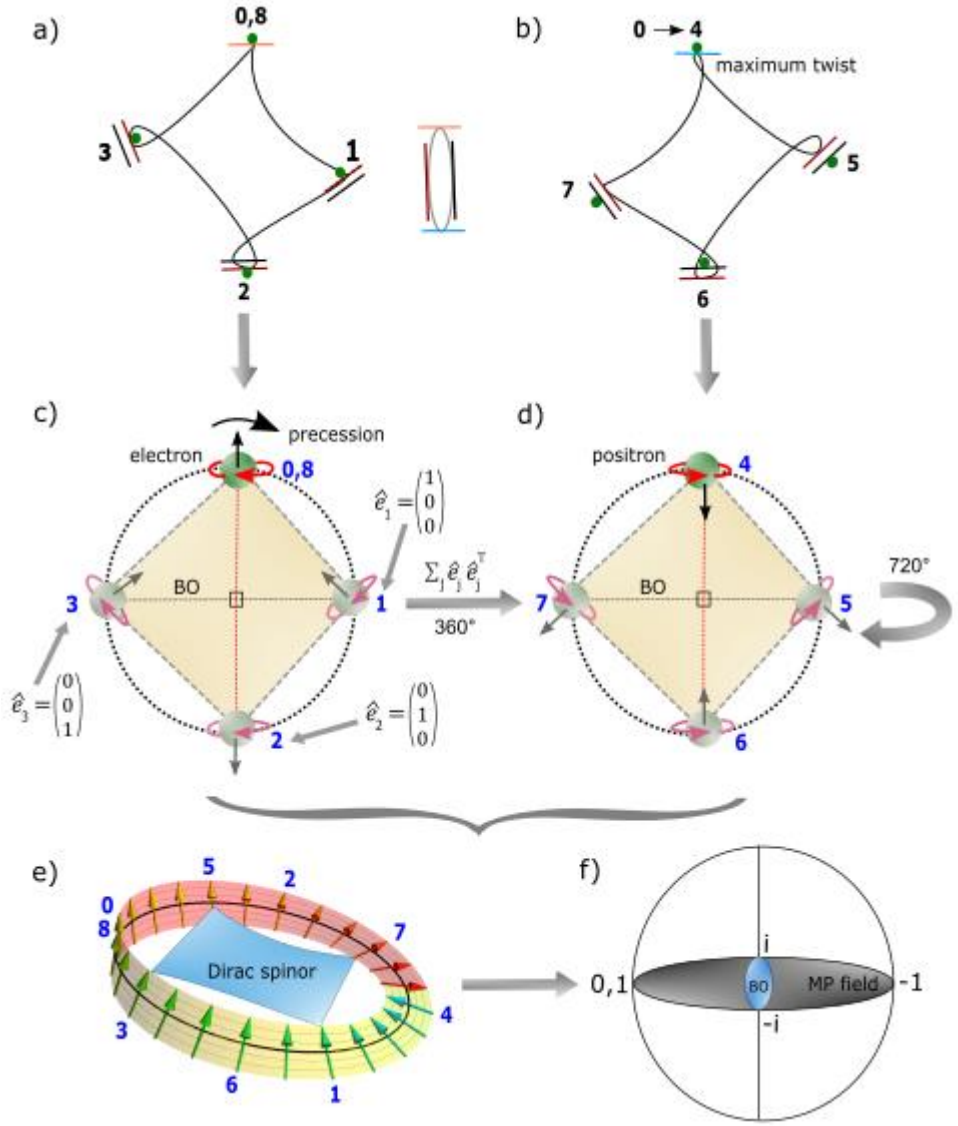

Figure 2. Exposition of Dirac belt trick. (a) An irreducible spinor field of close loop within a hemisphere is generated at spherical lightspeed with the electron's (green dot) shift in position of time reversal against clockwise precession of the MP model (Figure 1a). The position of the particle on a straight path (colored lines) is referenced to the MP field of elliptical shape (centered image). (b) Maximum twist is attained at position 4 as detectable energy and the unfolding process by another 360° rotation for a total of 720° rotation restores the electron at position 8 or 0 akin to Dirac belt trick. (c) Precession normalizes the loop to generate an electron of positive helicity or right-handedness. Spin up vector at the point-boundary correlates with the direction of precession. (d) At position 4, the electron flips to a positron of negative helicity or left-handedness. The spin down vector is in opposite direction to the direction of precession to begin the unfolding process. Transposition is attained at 720° rotation, $\sum_j \hat{e}_j \hat{e}_j^T = [e_i e_j] = c_{ij}^k e_k$ with c_{ij}^k is expansion coefficients, $\hat{e}_k$ is unit matrices and ij is electron-positron transition. (e) Irreducible spinor field at spherical lightspeed. Cancelation of charges at conjugate positions, 1, 3 and 5, 7 from on-shell momentum offers close loops of BOs into 3D of discrete form to stabilize the electron to only generate either spin up or spin down states respectively at position 0 and 4. The point of singularity at the center is evaded by shift in the electron orbit. The slight tilt at position 4 compared to position 0 is attributed to energy loss from the electron-positron transition in the form, $E = hv = g\beta B$. (f) Polarization of the model either horizontally or vertically with respect to the electron-positron pair, ±i at position 0 by 720° rotation generates qubits 0, 1 and hypercharge of –1 respectively at positions 0, 8 and 4. These are relevant to classical computing and

 doi:10.20944/preprints202210.0172.v12

accessibility to quantum computing for the nucleons are restricted by the chaotic system of envelop solitons at positions 2 and 6 (see also subsection 2d). Image (e) adapted from ref. [21].

The qubits 0 and 1 are assigned to the COM at positions 0 and 8, and hypercharge –1 to position 4 (e.g., Figure 1a). Such a notion can become relevant to classical computing, whereas quantum computing for nucleons mimicking the MP model is subjected to quantum chaos of butterfly effect assigned to envelop solitons at either position 2 or 6 encasing quantum critical point of the light-cone (see also subsection 2d). σ^i is assigned to oscillations from on-shell momentum of the BOs into n-dimensions (Figure 1d) for anticommutation relationship, $e^+(\psi) \neq e^-(\bar{\psi})$ of chiral symmetry (Figure 2c and 2d). The associated vector gauge invariance for the electron-positron transition exhibits the following relationships,

$$\psi_L \rightarrow e^{i\theta L}\psi_L \tag{17a}$$

and

$$\psi_R \rightarrow e^{i\theta L}\psi_R. \tag{17b}$$

The exponential factor, $i\theta$ refers to the position, i of the electron of a complex number and θ, is its angular momentum (e.g., Figure 1c). The unitary rotations of right-handedness (R) or positive helicity and left-handedness (L) or negative helicity are applicable to the electron transformation to Dirac fermion (e.g., Figure 2A in Appendix B). The process is confined to a hemisphere and this equates to spin 1/2 property of a complex spinor. Two successive rotations of the electron in orbit by clockwise precession of the MP field is identified by $i\hbar$. The chirality or vector axial current at the point-boundary is assigned to polarized states, ±1 of the model (Figure 1c). The helical symmetry from projections operators or nuclear isospin of z-axis acting on the spinors (Figure 2e) is,

$$P_L = \frac{1}{2}(1 - \gamma_5) \tag{18a}$$

and

$$P_R = \frac{1}{2}(1 - \gamma_5), \tag{18b}$$

where γ_5 is likened to thermal radiation of a black body. The usual properties of projection operators are: $L + R = 1$; $RL = LR = 0$; $L^2 = L$ and $R^2 = R$ (e.g., Figure 2a–d) consistent with CPT symmetry.

Wave function collapse. Dirac fermion or spinor is denoted $\psi(\mathbf{x})$ in 3D Euclidean space and it is superimposed onto the MP model of 4D space-time, $\psi(\mathbf{x},t)$ by clockwise precession (Figure 3a). The latter resembles Minkowski space-time and consists of a light-cone dissected by z-axis as arrow of time into asymmetry (Figure 1b). The former includes both positive and negative curvatures of non-Euclidean space (e.g., Figure 2a,b) normalized to straight paths of Euclidean space (Figure 2c,d). These are of non-abelian Lie group (see subsection 2c) imposed on the surface of the spherical MP model somewhat mimicking Poincaré sphere. The Dirac four-component spinor, $\psi = \begin{pmatrix} \psi_0 \\ \psi_1 \\ \psi_2 \\ \psi_3 \end{pmatrix}$ is attributed to positions 0 to 3 of conjugate pairs in 3D space. Convergence of positions 1 and 3 at either position 0 or 2 is relevant to the equivalence principle based on general relativity and is relevant to Euclidean geometry. The quantum aspect of de Sitter space by geodetic clockwise precession is balanced out by anti-de Sitter form of the electron transition in its orbit of time reversal due to gravity. For the irreducible spinor represented by the MP model, gravity is assigned to a gyroscopic geometry. Any light paths tangential to the point-boundary of BOs into n-energy manifolds is expected to mimic Fourier transform along the principle axis or z-axis of the MP field as time axis in asymmetry and this is equivalent to wave function collapse (Figure 3b). Constraining the electron's position along the z-axis offers the uncertainty principle with on-shell momentum linked to BO. The generated wave amplitudes from BOs levitation into n-dimensions can relate to a typical hydrogen emission spectrum

Preprints.org (www.preprints.org) | NOT PEER-REVIEWED | Posted: 22 August 2024 doi:10.20944/preprints202210.0172.v12

for external light-matter coupling with the electron in orbit (Figure 3c). In this case, wave function collapse of probabilistic distribution by Born's rule, $|\psi|^2$, is applicable to excitation of the model.

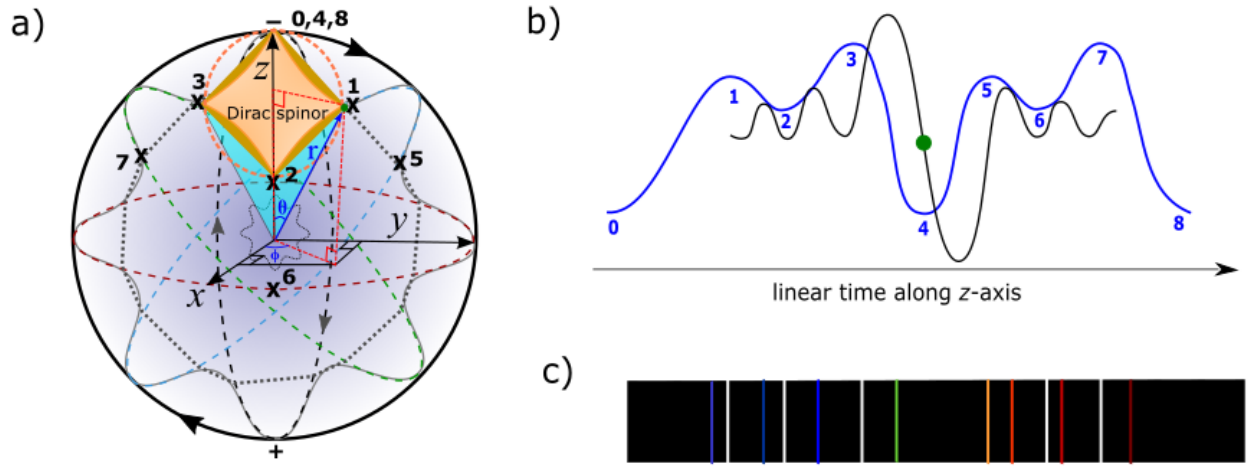

Figure 3. Wave function collapse. (a) Irreducible Dirac spinor is defined by vector space superimposed on Poincaré sphere. It consists of both Euclidean (straight paths) and non-Euclidean (negative and positive curves) spaces. Clockwise precession by geodesic motion induces a circle at 360° rotation to the negative curves at positions 0 to 3 (e.g., Figure 2c). The polar coordinates (r, θ, Φ) are linked to a light-cone (navy colored). Position 6 is projected inwards from position 2. (b) By on-shell momentum of BO with respect to the electron position in transition is applicable to Fourier transform (blue wavy curve) into linear time. Positions 2 and 6 constrains the reach of singularity. Zooming in towards real particle emergence at position 0 presents the Heisenberg uncertainty principle (black wavy curve) of superposition states. (c) The particle shifts in position and levitation of BOs into n-dimensions (Figure 1d) can somehow translate to a typical hydrogen emission spectrum. The amplitudes by Fourier transform are shown by white spectral lines and the uncertainty principle with respect to the particle property by colored spectral lines. .

⇒ **Quantized Hamiltonian.** Two ansatzes adapted from Equation (14) are given by,

$$\psi = u(\mathbf{p})e^{-ip.x}, \tag{19a}$$

and

$$\psi = v(\mathbf{p})e^{ip.x}, \tag{19b}$$

where outward project of spin at positions 5, 7 is represented by v and inward projection at positions 1, 3 by u (e.g., Figure 2c,d). By linear transformation, the hermitian plane wave solutions form the basis for Fourier components in 3D space (Figures 1d and 3b). Decomposition of quantized Hamiltonian [22] ensues as,

$$\psi(x) = \frac{1}{(2\pi)^{3/2}} \int \frac{d^3}{2E_{\mathbf{p}}} \sum_s \left(a_{\mathbf{P}}^s u^s(p) e^{-ip.x} + b_{\mathbf{P}}^{s\dagger} v^s(p) e^{ip.x} \right), \tag{20a}$$

where the constant, $\frac{1}{(2\pi)^{3/2}}$ is attributed to the dissection of BOs along z-axis. Its conjugate form is by,

$$\bar{\psi}(x) = \frac{1}{(2\pi)^{3/2}} \int \frac{d^3}{2E_{\mathbf{p}}} \sum_s \left(a_{\mathbf{P}}^{s\dagger} \bar{u}^s(p) e^{ip.x} + b_{\mathbf{P}}^s \bar{v}^s(p) e^{-ip.x} \right). \tag{20b}$$

The coefficients $a_{\mathbf{P}}^s$ and $a_{\mathbf{P}}^{s\dagger}$ are ladder operators for u-type spinor and $b_{\mathbf{P}}^s$ and $b_{\mathbf{P}}^{s\dagger}$ for v-type spinor at n-dimensions of BOs by levitation (e.g., Figure 1d). These are related to Dirac spinors of two spin states, ±1/2 with $\bar{v}^s$ and $\bar{u}^s$ as their antiparticles. Dirac Hamiltonian of one-particle quantum mechanics relevant to the MP model of hydrogen atom type is,

 doi:10.20944/preprints202210.0172.v12

$$H = \int d^3x\psi^\dagger(x)[-i\gamma^0\gamma.\boldsymbol{\nabla} + m\gamma^0]\,\psi(x). \tag{21}$$

The quantity in the bracket is provided in Equation (3). By parity transformation, the observable and holographic oscillators are canonically conjugates (e.g., Figure 2c,d). The associated moment

$$\pi = \frac{\partial\mathcal{L}}{\partial\psi} - \bar{\psi}i\gamma^0 = i\psi^\dagger. \tag{22}$$

With z-axis of the MP field assuming time axis in asymmetry (Figure 1c), V-A currents are projected in either x or y directions in 3D space comparable to Fourier transform (e.g., Figure 3b). These assume the relationships,

$$\left[\psi_\alpha(\mathbf{x},t),\psi_\beta(\mathbf{y},t)\right] = \left[\psi_\alpha^\dagger(\mathbf{x},t),\psi_\beta^\dagger(\mathbf{y},t)\right] = 0, \tag{23a}$$

and its matrix form,

$$\left[\psi_\alpha(\mathbf{x},t),\psi_\beta^\dagger(\mathbf{y},t)\right] = \delta_{\alpha\beta}\delta^3(\mathbf{x}-\mathbf{y}), \tag{23b}$$

where α and β denote the spinor components of ψ. Equations (23a) refers to unitarity of the model and Equation (23b) is assumed by the electron-positron transition about the manifolds of BOs in 3D space (Figure 1d). The ψ independent of time in 3D space obeys the uncertainty principle with respect to the electron's position, $\mathbf{p}$ and momentum, $\mathbf{q}$, as conjugate operators (Figure 1c). The commutation relationship of $\mathbf{p}$ and $\mathbf{q}$ is,

$$\left\{a_{\mathbf{p}}^r, a_{\mathbf{q}}^{s\dagger}\right\} = \left\{b_{\mathbf{p}}^r, b_{\mathbf{q}}^{s\dagger}\right\} = (2\pi)^3\delta^{rs}\delta^3(\mathbf{p}-\mathbf{q}). \tag{24}$$

Equation (24) incorporates both matter and antimatter and their translation to linear time (Figure 3b). The electron as a physical entity generates a positive-frequency such as,

$$\langle 0|\psi(x)\bar{\psi}(y)|0\rangle = \langle 0\,| \int \frac{d^3p}{(2\pi)^3}\frac{1}{\sqrt{2E_{\mathrm{p}}}}\sum_r a_{\mathrm{p}}^r u^r(p)e^{-ipx}$$

$$\times \int \frac{d^3q}{(2\pi)^3}\frac{1}{\sqrt{2E_{\mathrm{q}}}}\sum_s a_{\mathrm{q}}^{s\dagger}\bar{u}^s(q)e^{iqy}\;|\,0\rangle. \tag{25}$$

Equation (25) could explain the dominance of matter (electron) over antimatter based on the conceptualization process of Dirac fermion (e.g., Figure 2a,b).

⇒ **Non-relativistic wave function.** Observation by light-matter interaction allows for the emergence of the model from the point-boundary at Planck length. Subsequent energy shells of BOs at the n-levels by excitation accommodates complex fermions, ±1/2, ±3/2, ±5/2 and so forth (Figure 4a). The orbitals of 3D are defined by total angular momentum, $\vec{J} = \vec{l} + \vec{s}$ and this incorporates both orbital angular momentum, l and spin angular momentum, s (Figure 4b). These are aligned with Schrödinger wave function (e.g., Figure 1c). The reader is also referred to Appendices, A, B and C. Within a hemisphere, the model is transformed to a classical oscillator. By clockwise precession, a holographic oscillator from the other hemisphere of the MP field remains hidden. One oscillator levitates about the other (Figure 4b) and both are not simultaneously accessible to observation by Fourier transform (e.g., Figure 3b). Levitation of on-shell momentum of BO into n-levels by

Preprints.org (www.preprints.org) | NOT PEER-REVIEWED | Posted: 22 August 2024 doi:10.20944/preprints202210.0172.v12

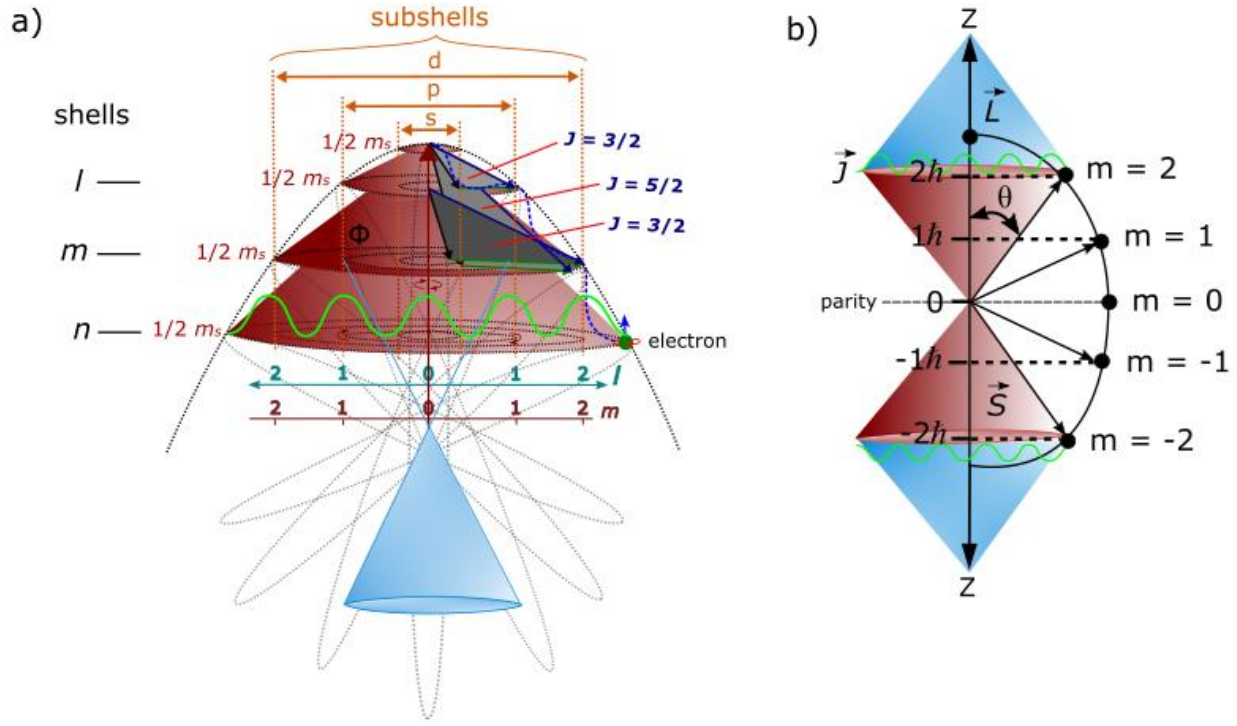

Figure 4. Light-MP model coupling. (a) To an external observer, the topological point-boundary provides the origin for the emergence of the oscillator (maroon light-cones). Total angular momentum, $J_z = S + L$ is minimal with S and L in opposite directions. Levitation of BOs into n-dimensions from n to k coalesces at the point-boundary of COM assigned to electron-positron transition at position 0. The BOs in degeneracy, Φ_i (see also Figure 1d) can accommodate Fermi-Dirac statistics (green wavy curve) and possibly Fock space for non-relativistic many-particle systems if multielectron are assigned to multiple MP fields. The observable oscillator is partitioned at an infinite boundary towards the center of the MP field and is equivalent to atomic wave of linear time. The blue light-cone is from the perspective of the observer at the center and is relevant to Schrödinger wave function (e.g., Figure 1c) with subshells assigned to spectroscopic notations at n-dimensions. (b) The emergence of quantized magnetic moment, $\pm J_z = m_j\hbar$ from the point-boundary (maroon light-cones) levitates about the internal frame of the model (blue light-cones). Parity transformation for the conjugate pairs is confined to a hemisphere (e.g., Figure 2a,b) and it is related to z-axis of nuclear isospin. Minimal scatterings (green wavy curves) are applicable to light-MP model interactions along the BOs for the eigenfunction, $\vec{J} = \vec{L} + \vec{S}$.

disturbance can be pursued for Fermi-Dirac statistics if these equate to fermions. The point-boundary at the vertex of MP field at position 0 of COM is assigned to ZPE and both vertices constrain vacuum energy with its perturbation by precession. The $\pm\vec{J}$ splitting (Figure 4a) applies to Landé interval rule for the electron of weak isospin and this can somehow relate to lamb shift based on the subshells of BOs by levitation into n-dimensions (e.g., Figure 1d). Such a scenario is similar to how vibrational spectra of a harmonic oscillator for diatoms like hydrogen molecule incorporates rotational energy levels (Figure 4a). The difference of the classical oscillator to the quantum scale is the application of Schrödinger wave equation (e.g., Figure 1c).

⇒ **Weyl spinor.** The light-cone within a hemisphere accommodates both matter and antimatter by parity transformation (Figure 4a,b). It is described in the form,

$$\psi = \begin{pmatrix} \psi_0 \\ \psi_1 \\ \psi_2 \\ \psi_3 \end{pmatrix}. \tag{26}$$

 doi:10.20944/preprints202210.0172.v12

Equation (26) corresponds to spin up fermion, a spin down fermion, a spin up antifermion and a spin down antifermion (e.g., Figure 2c,d). By forming its own antimatter, Dirac fermion somewhat resembles Majorana fermions. It is difficult to observe them simultaneously due to wave function collapse long z-axis of linear time (e.g., Figure 3b). Non-relativistic Weyl spinor of a pair of light-cones in 4D space-time are relevant to Schrödinger wave equation in 3D space (Figures 1c, 3a and 4a). These are defined by reduction of Equation (26) to a bispinor in the form,

$$\psi = \begin{pmatrix} u_+ \\ u_- \end{pmatrix}, \tag{27}$$

where $u_\pm$ are Weyl spinors of chirality with respect to the electron position. By parity operation, $x \rightarrow x' = (t, -\mathbf{x})$, qubits 1 and −1 are generated at the vertices of the MP field (e.g., Figure 1c). Depending on the reference point-boundary of the BO (Figure 1d), the exchanges of left- and right-handed Weyl spinor assumed the process,

$$\begin{pmatrix} \psi'_L \\ \psi'_R \end{pmatrix} = \begin{pmatrix} \psi_R(x) \\ \psi_L(x) \end{pmatrix} \Rightarrow \begin{matrix} \psi'(x') = \gamma^0\psi(x) \\ \bar{\psi}'(x') = \bar{\psi}(x)\gamma^0. \end{matrix} \tag{28}$$

Conversion of Weyl spinors to Dirac bispinor, $\xi^1\ \xi^2$ are of transposition state (e.g., Figure 2c and 2d)). The two-component spinor, $\xi^1\ \xi^2 = 1$ are normalized at the point-boundary at position 0 of the spherical model (Figure 1a).

⇒ **Lorentz transformation.** The Hermitian pair, $\psi^\dagger\psi$ of Dirac fermion based on Equation (27) undergo Lorentz boost and translate the BOs into n-levels (Figure 1d) of the form,

$$u^\dagger u = (\xi^\dagger\sqrt{p.\sigma},\ \xi\sqrt{p.\bar{\sigma}}\,.\begin{pmatrix} \sqrt{p.\sigma}\xi \\ \sqrt{p.\bar{\sigma}}\xi \end{pmatrix},$$

$$= 2\mathrm{E_P}\xi^\dagger\xi\,. \tag{29}$$

The corresponding Lorentz scalar applicable to scattering from on-shell momentum tangential to the BOs (Figure 1d) is, <

$$\bar{u}(p) = u^\dagger(p)\gamma^0. \tag{30}$$

Equation (30) is referenced to z-axis of the MP field as time axis and is relevant to Fourier transform into linear time. By identical calculation to Equation (29), the Weyl spinor is,

$$\bar{u}u = 2m\xi^\dagger\xi, \tag{31}$$

Both Weyl spinor of a light-cone (Figure 4a) and Majorana fermion are indistinguishable from Dirac spinor for light-matter interaction confined to position 0 (e.g., Figure 1a).

⇒ **Electroweak symmetry breaking.** Based on the dynamics of the MP model described in section 2, its disturbance from either coupling of external light or MP models can somewhat generate electroweak symmetry breaking. Conservation of the model is considered from ejection of electron of weak isospin to hypercharge of ±1 assigned to position 0 of COM (Figure 5a,b) (see also subsection 2d). The emergence of particle-hole symmetry mimicking the electron-positron transition will exhibit variation in the electrostatic force with the proton. This could contribute to proton radius puzzle if the particle-hole in orbit dictates z-axis of the MP field of nuclear isospin at precession. Any adjustments by the proton to accommodate changes in charge and mass is expected to break CPT symmetry such as for electroweak symmetry breaking for beta decay, $n^0 \rightarrow p^+ + W^- \rightarrow uud + e^- + \bar{\nu}$ (Figure 6). Observation becomes deterministic into forward time and particle property is assigned tangential to BOs into n-dimensions for on-shell momentum. The neutrino types (e.g., $\bar{\nu}$) of helical property would mimic the electron-positron transition and these can be generated at positions 1 and 3 with trivial shift in z-axis, $\langle z|z'\rangle = \delta(z - z')$ by precession (Figure 1d). By on-shell momentum ($p^2 = m^2$), particles acquire energy, γ or $\frac{-ig_{uv}}{p^2}$ and this sustains Einstein mass-energy equivalence of the form,

Preprints.org (www.preprints.org) | NOT PEER-REVIEWED | Posted: 22 August 2024 doi:10.20944/preprints202210.0172.v12

$$E^2 - |\vec{p}|^2c^2 = m^2c^2. \quad (32)$$

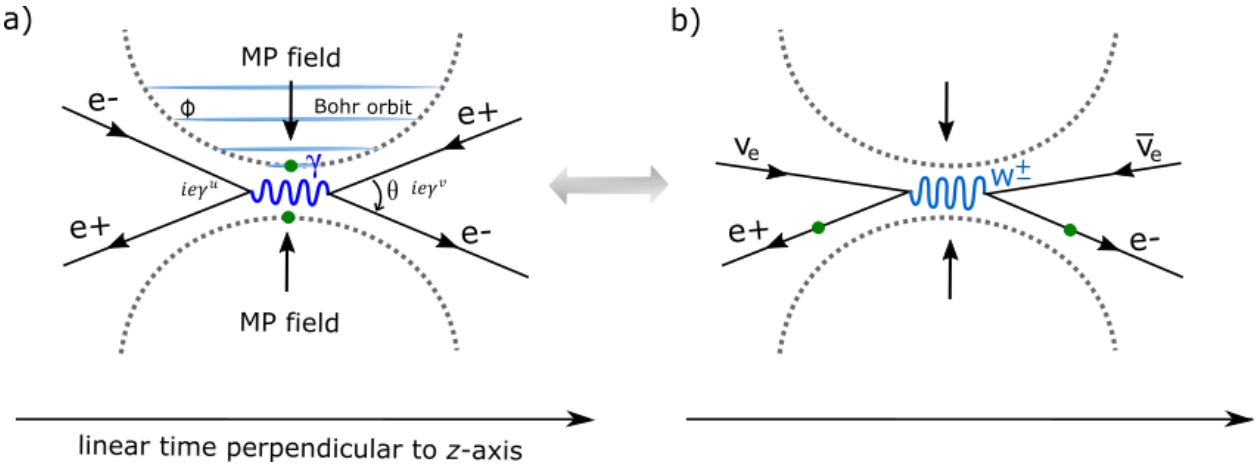

Figure 5. Feynman diagrams of MP models coupling. (a) Two electrons (green dots) or their particle-hole symmetries at the vertices of the MP models may undergo either repulsion or attraction when approaching each other. (b) Ejection of the electron or positron would induce weak particle-hole isospin. The COM of ZPE at the vertices can account for both boson and fermion types such as neutrinos and antineutrinos of helical property mimicking the electron-positron pair (e.g., Figure 2c,d).

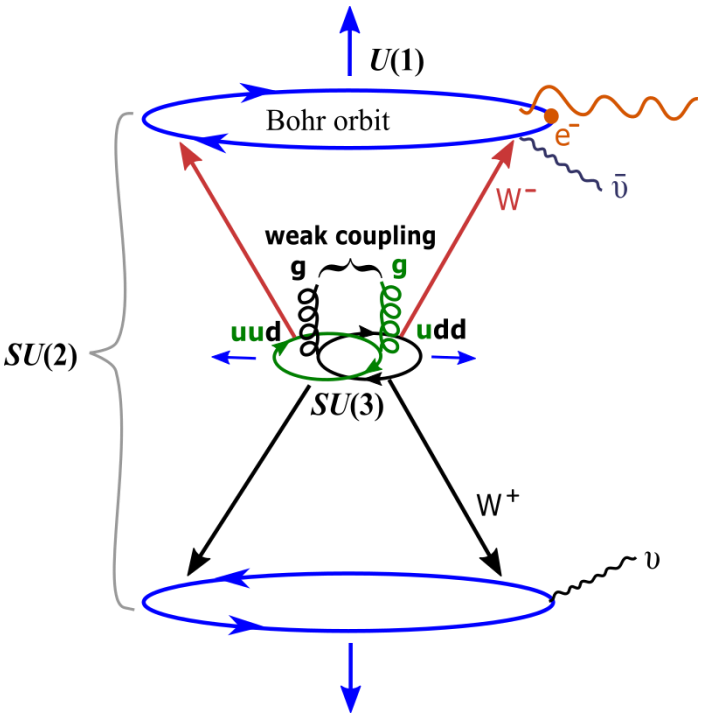

Figure 6. A hypothetical scenario of beta decay from an energized MP model. The proton and neutron are of doublet MP fields of 4D that transforms to 8D by precession. The charge and color flavor of quarks from exchanges by gluons are short range from on-shell momentum tangential to the BO. The symbols, u = up quark, d = down quark and g = gluon. Note, $W^{\pm}$ bosons can align to the light-cones with respect to *z*-axis of the MP field (blue arrows) as nuclear isospin.

Translation by wave function collapse is normalized to the *z*-axis (Figure 3b) for particles possessing angular momenta, $ieγ^u$, $ieγ^v$ such as vector bosons, $W^{\pm}$ with respect to a light-cone of time invariance (Figure 6). If spin 1 and spin 0 particles are assigned to the COM of ZPE at the point-

 doi:10.20944/preprints202210.0172.v12

boundary of a classical oscillator (Figure 4a), hypercharge BOs by levitation into n-dimensions of Minkowski space-time (Figure 1d) are relevant to the emergence of leptons. Higgs-like boson, $H°$ assigned to COM is included in the first term of its field of a scalar quantity, $V(\phi) = m_H^2\phi^2 + \lambda\phi^4$ for proton-proton collisions mimicking the MP models. The second term is applicable to positions 1 and 3 by precession into space-time with the emergence of measureable quantity, ϕ about horizontal x-axis (Figure 1a). The y-axis consists of imaginary potential, ϕ and both axes are normalized to z-axis of the MP field as time axis in asymmetry (e.g., Equations (23a and 23b)). The constriction of the model towards infinite n-dimensions at high energy intercepts the baseline of the pair of hemispheres. The electron at positions 2 and 6 form envelop solitons from merging of the hemispheres (see subsection 2d). Their transformation to Nambu-Goldstone boson is expected and by relaxation, $H°$ emerges at the vertex of the MP field. Comparable to instanton magnetic monopoles at the vertices (subsection 2d), the boson is not transferrable when confined to the MP field of Dirac string resembling a little magnet. The stochastic wave amplitudes from envelop solitons of the chaotic system is relevant to the emergence of butterfly effect are relegated to electron-positron transition at positions 2 and 6 of interchangeability to linear light paths at low energy. Thus, accessibility to signals from the nucleons at singularity or quantum critical point for quantum critical region defined by the light-cone is restricted. Such a notion can become important to quantum computing for nucleons mimicking the MP model (Figure 6), if classical qubits of 0, 1 and –1 are assumed by the electron-positron transition (e.g., Figure 2f).

In high energy physics, the electron or its particle-hole by ejection due to ionization is expected to instigate asymptotic freedom from proton-proton collision mimicking coupling of MP models (e.g., Figure 5a and 5b). High luminosities are expected from integration of particle-hole and proton with coupling to similar types. Stochastic waves emanating from envelop solitons at positions 2 and 6 can align with S-matrix and allow for confinement of quark flavor and color charge of ±1/3 spin. The link of the quark model to COM is assumed along z-axis of the MP field as nuclear isospin or time axis in asymmetry and this is link to $H°$ of ZPE. These explanations offer an alternative interpretation of electroweak symmetry breaking with variations in mass and charge for a plethora of particles from on-shell momentum of BO by levitation into n-dimensions (e.g., Figure 1d). The particles' relationships to vectors, matrices and tensors are alluded in the text and further demonstrated in Figure 2A (Appendix B). Such an undertaking looks promising to combine nuclear physics, high and low energies physics for electroweak breaking of SU(3) x SU(2) x U(1) symmetry (Figure 6). For example, in nuclear radiation, multiple MP fields can be assigned to multielectron atoms by the conservation of the MP models irrespective of the atom types. Thus, if U(1) is assigned to COM of ZPE at the spherical point-boundary (see subsections 2b and 2d), then SU(2) is described by Lie group (subsection 2c) and Dirac field theory offered in this section. SU(3) is linked to z-axis of the MP field as nuclear isospin dissecting miniature doublet MP models of 4D to form 8D of the quark model (Figure 6). Any deviations in the magnetic moment of the electron is translated by levitation of BO into n-dimensions with link to energy subshells (e.g., Figure 4a) and this can offer some insights into the fine-structure constant, $a = \frac{e^2}{\hbar c} = \frac{e^2}{4\pi} \approx \frac{1}{137}$ such as lamb shift and this is relevant to the pursuits in quantum electrodynamics.

4. Conclusion

The dynamics of the MP model of 4D space-time offered in this study allows for the transformation of the electron of hydrogen atom type to Dirac fermion of a complex four-component spinor. The model consists of an electron in orbit of time reversal in an elliptical MP field of Dirac string undergoing clockwise precession to generate a spherical geometry relevant to both Minkowski and Euclidean space-times. The electron-positron transition confined to a hemisphere of time invariant sustains CPT symmetry and this appears consistent with Dirac belt trick and basic interpretations of quantum mechanics and Lie group. The point-boundary at the vertex of the MP field from electron-positron transition is assigned to COM and this is relevant for the emergence of ZPE and instanton magnetic monopoles. Envelop solitons of chaotic classical system are assigned to electron-positron transition at the horizontal line of precession dissecting the nucleus. These

 doi:10.20944/preprints202210.0172.v12

dynamics of the MP model are compatible with Dirac field theory and some of its related components like wave function collapse, quantized Hamiltonian, non-relativistic wave function, Weyl spinor, Lorentz transformation and electroweak symmetry breaking mechanism. Though MP model remains a speculative tool, it can become important towards defining the fundamental state of matter and its field theory as demonstrated in this study and this warrants further investigations.

Data Availability Statement: The modeling data attempted for the current study are available from the corresponding author upon reasonable request.

Competing financial interests: The author declares no competing financial interests.

Appendix A—Mathematical property of Schrödinger wave equation

The Schrödinger equation cannot be derived similar to Newton's law of gravity. Its mathematical property can be plotted [23] beginning with the normalized sine wave function,

$$\psi = Asin\frac{2\pi x}{\lambda}, \qquad (1A)$$

where A is the amplitude shown in Figure 1A. Its second derivation is,

$$\frac{d^2\psi(x)}{dx^2} == \frac{-4\pi^2}{\lambda^2}\psi(x). \qquad (2A)$$

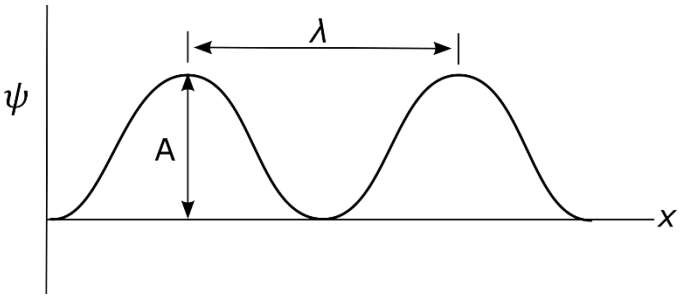

Figure 1A. Translation of a sine wave function along x-axis.

Velocity, v can be calculated from total energy in the form,

$$v^2 = \frac{2(E-V)}{m}, \qquad (3A)$$

where V is potential energy and kinetic energy is, $\frac{1}{2}mv^2$. Taking the squared function of de Broglie relationship becomes,

$$\lambda^2 = \frac{h^2}{m^2v^2}. \qquad (4A(i))$$

By substitution from Equation (3A), Equation (4A(i)) can be rewritten as,

$$\lambda^2 = \frac{h^2}{2m(E-V)}. \qquad (4A(ii))$$

By substitution into Equation (2A), this becomes,

$$\frac{d^2\psi(x)}{dx^2} == \frac{-8m\pi^2}{h^2}(E-V)\psi(x). \qquad (5A(i))$$

An alternative form of Equation (5A(i)) is,

$$-\frac{\hbar}{2m}\frac{\partial^2}{\partial x^2} + V\psi(x) = \frac{p^2}{2m}\psi(x) = E\psi(x). \qquad (5A(ii))$$

Preprints.org (www.preprints.org) | NOT PEER-REVIEWED | Posted: 22 August 2024 doi:10.20944/preprints202210.0172.v12

By first derivation of space-time due to clockwise precession of the MP model (Figure 1c), Equation (5A(ii)) is given by,

$$i\hbar\frac{\partial}{\partial t}(\psi(\vec{r})\theta(t) = E\psi. \qquad (5A(iii))$$

In this way, the model offers physical meaning to Schrödinger wave equation as an eigenvalue of ψ similar to Newton's law of gravity with the electron of isospin represented by, i or $2m$.

Appendix B—Basis of vectors, matrices, tensors and Fourier transform

The physicality of the complexity of Dirac four-component spinor can somehow relate to the geometric MP model. The BOs provide the basis for vector to multivector by levitation into n-dimensions or n-energy levels along the z-axis (Figure 2A). By rotation, the BOs generate both spin

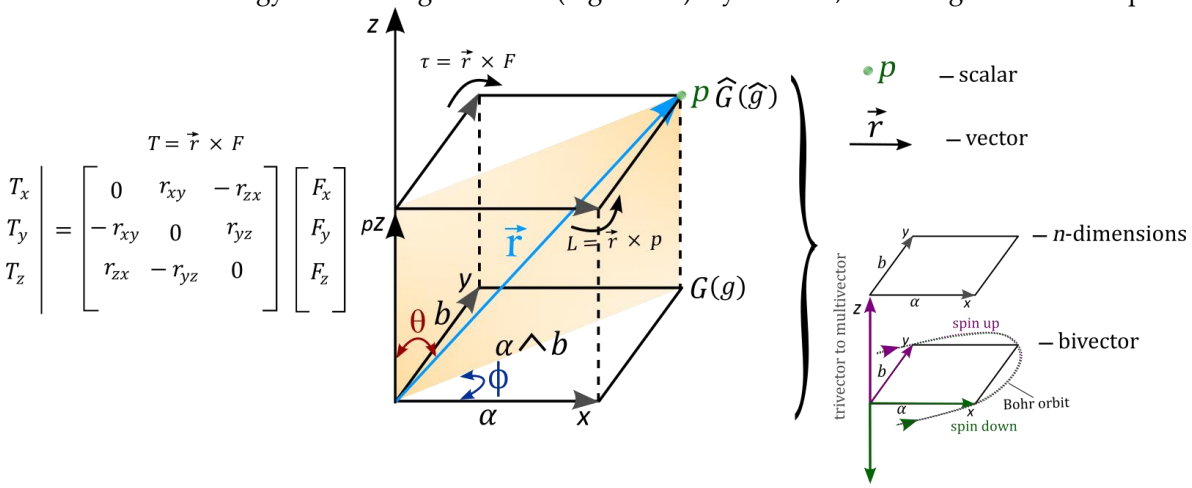

Figure 2A. The basis of vectors to multivectors, matrices, tensors and Fourier transform. The vectors are aligned with either spin up or spin down by rotation of the BO. Translation along z-axis of nuclear isospin provides trivectors to multivector into n-dimensions by levitation of BOs of unidirectional. The matrices are related to tensors along z-axis by Fourier transform for the commutation, pZ to Z (see text for details). The $\vec{r}$ is a four 3-fold rotational axis (shaded orange plane) in 3D of the box and is applicable to Fourier transform (e.g., Figure 3b). It mimics a 4-gradient Dirac operator, ∇ for vectors to multivector into n-dimensions of the box (see also red rectangle in Figure 1c). Rotation into forward time, $\tau = \vec{r} \times F$ is by clockwise precession and this insinuates spin up with the unfolding process for spin down by, $L = \vec{r} \times p$. The spin rotation matrices applicable to Clifford algebra are shown to the left. The half-integer spins of SU(2) group provide double cover (bivector) with shift in both θ and ϕ into n-dimensions by levitation of BOs. This is relevant to the Lie group ladder operators, $G(g)$ and $\hat{G}(\hat{g})$. Some key features of the dimensional box are expounded to the right.

up and spin down in correspondence to the principle axis of the MP field as time axis in asymmetry. The manifold of BOs can be assigned to a box (Figure 2A). The rotation by $\vec{r}$ is a four 3-fold axis in 3D and its matrices are defined by Cartesian coordinates, x, y and z. These are related to shift in both θ and Φ as double cover of SU(2) for vector to multivectors assumed within the BOs. They are applicable to the Lie group ladder operators, $G(g)$ and $\hat{G}(\hat{g})$ of 3D space and 4D space-time. By linearization akin to Fourier transform (e.g., Figure 3b), the boxes of isomorphism consisting of BOs by levitation and these are translated along the z-axis of the MP field (Figure 2A). The BO of bivector field is related to z/pz of integers modulo p of prime. The shift along z-axis of isospin from vertices of the MP field of Dirac string is commutative (Figure 2A) and any changes by precession is trivial. The MP model of irreducible representation, Π is given by [21],

$$\rho(g) = [\Pi(\hat{g})], \qquad (6A)$$

where ρ is composed of algebraic structure (pz, $+p$ and xp) for vectorization, V into p-dimensional space defined by $\alpha \wedge b$ (Figure 2A). The two operators, T_a and S_a acting on V are

 doi:10.20944/preprints202210.0172.v12

$$(T_a f)(b) = f(b-a) \qquad (7\text{A(i)})$$

and

$$(S_a f)(b) = e^{2\pi i a b} f(b), \qquad (7\text{A(ii)})$$

where T is identified by the rotational matrices, $T = \vec{r} \times F$ (Figure 2A) and S_a is the shift in frequency in space along z-axis (e.g., Figure 3b). These intuitive demonstrations somehow provide a geometry perspective to the MP model with its relevance to the Lie group and QFT in terms of Dirac field theory elaborated in the article (see subsection 2c and section 3).

Appendix C—Vector modelling of the MP model

Schrödinger wave equation forms the basis of quantum mechanics and offers satisfactory explanations to account for probability distribution or orbitals of subatomic particles like electrons in the atom. However, quantum mechanics cannot account for the combination of orbital angular momenta, spin angular momenta and magnetic moments of valence electrons observed in atomic spectra. Russell-Saunders orbital-spin (L-S) coupling ensues by Clebsch-Gordon series such as for the eigenvalue of total angular momentum, $\vec{J} = \vec{l} + \vec{s}$, and this incorporates eigenvalues of both orbital angular momentum, l and spin angular momentum, s.

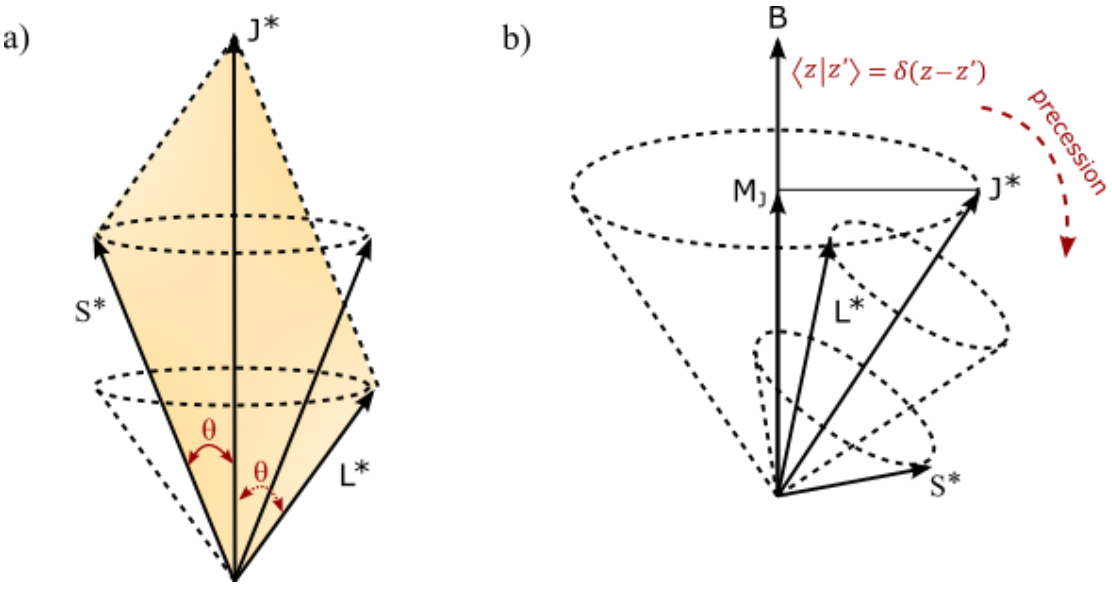

Figure 3A. Vectors of orbital angular momentum. (a) Vectors **L** and **S** precess about this resultant **J**. In other words, any precession affecting **L** and **S** in the form, $\langle z|z'\rangle = \delta(z-z')$ is reduced to the MP field of magnetic property such as Dirac string along z-axis. The shaded area of bivector from Figure 2A is extended to the point-boundary of the MP model (see also Figure 4a). (b) Vector J of the MP field precesses in correspondence to applied external magnetic field **B**. Both images are adapted from ref. [24].

From the emergence of the oscillator at the point-boundary (Figure 4a), levitation of BOs into n-dimensions can cater for both the resultant orbital angular momentum, **L** and resultant spin angular momentum, **S**, where spin-orbit interaction is related to constant shift in the electron position. Complete rotation towards the point-boundary by Dirac process is twice, 2π and the positron-electron transition is related to h. The lone valence electron of the MP model akin to hydrogen atom by precession takes the form,

$$|l| = \sqrt{l_i(l_i+1)}\hbar, \qquad (8\text{A(i)})$$

 doi:10.20944/preprints202210.0172.v12

where i is equal to the subshells (Figure 4a). For example, $n = 2$ is split into s and p orbitals with each one accommodating spin 1/2 and from electron-positron transition of Dirac process at spherical lightspeed (Figure 1a), this equates to ±1/2 spin in accordance with Pauli exclusion principle. The total angular momentum, $\vec{J} = l \pm \frac{1}{2}$, is $\frac{3}{2}$ and $\frac{1}{2}$ at $n = 2$, $l = 1$. The former is assumed from the summation of spin, 1/2 + 1/2 + 1/2 from combined s and p subshells by $n_2 + n_1 = \frac{3}{2}$, when both orbital and spin angular momenta are aligned in the same direction (Figure 4b). It also provides the magnitude of **S**. The latter of low energy from $n_2 - n_1 = \frac{1}{2}$ in the form, 1/2 + 1/2 − 1/2 and is assigned to p orbital by cancelling out 1s orbital. This does not consider the orientation such as of the p subshells by levitation into n-dimensions (e.g., Figure 4a). The corresponding **L** from the combination of $\sum l_i$ in a complete loop of BO at n-dimension is,

$$|\mathbf{L}| = \sqrt{\mathbf{L}_n(\mathbf{L}_n + 1)}\hbar, \qquad (8A(ii))$$

where the values of 0, $\sqrt{2}\hbar$ and $\sqrt{6}\hbar$ are generated at $n = 0$ to $n = 2$. Their projection with respect to z-axis for the irreducible MP field is,

$$|\mathbf{L_Z}| = M_L\hbar. \qquad (8A(iii))$$

Equation (8A(iii)) is applicable to the light-cone and the same is projected for $\vec{J}$ such as,

$$J_Z = m_l\hbar, \qquad (9A(i))$$

where m_l can take $(2l + 1)$ values in both equations as eigenfunciton of M_L. Both **S** and **L** combine to generate **J** in the form,

$$\mathbf{J} = \mathbf{L} + \mathbf{S}. \qquad (9A(ii))$$

Distinction of **L** and **S** are provided in Figure 4b and the orientations by precession are applicable to M_L. These explanations can possibly account for odd fermion spin types such as, $\frac{1}{2}, \frac{3}{2}, \frac{5}{2}$ noted for Zeeman effect (e.g., Figure 4a) and also lamb shift from the electron-positron transition in discreet form (e.g., Figure 3c). In this case, the electron is of weak isospin and z-axis is applicable to nuclear isospin. Both are linked to BOs into n-dimensions by levitation and these are subjected to the twisting and unfolding process by Dirac process (Figure 1a and 1b).

References

1. Peskin, M. E. & Schroeder, D. V. *An introduction to quantum field theory*. Addison-Wesley, Massachusetts, USA (1995). pp 13–25, 40–62.
2. Alvarez-Gaumé, L. & Vazquez-Mozo, M. A. Introductory lectures on quantum field theory. *arXiv preprint hep-th/0510040* (2005).
3. Pawłowski, M. et al. Information causality as a physical principle. *Nature* **461**(7267), 1101-1104 (2009).
4. Henson, J. Comparing causality principles. *Stud. Hist. Philos M. P*, **36**(3), 519-543 (2005).
5. Nelson, E. Derivation of the Schrödinger equation from Newtonian mechanics. *Phys. Rev.* **150**(4), 1079 (1966).
6. Li, Z. Y. Elementary analysis of interferometers for wave—particle duality test and the prospect of going beyond the complementarity principle. *Chin. Phys. B* **23**(11), 110309 (2014).
7. Rabinowitz, M. Examination of wave-particle duality via two-slit interference. *Mod. Phys. Lett. B* **9**(13), 763-789 (1995).
8. Rovelli, C. Space is blue and birds fly through it. *Philos. Trans. Royal Soc. Proc. Math. Phys. Eng.* **376**(2123), 20170312 (2018).
9. Perkins, D. H. Proton decay experiments. *Ann. Rev. Nucl. Part. Sci.* **34**(1), 1-50 (1984).
10. Sun, H. Solutions of nonrelativistic Schrödinger equation from relativistic Klein–Gordon equation. *Phys. Lett. A* **374**(2), 116-122 (2009).
11. Oshima, S., Kanemaki, S. & Fujita, T. Problems of Real Scalar Klein-Gordon Field. *arXiv preprint hep-th/0512156* (2005).
12. Bass, S. D., De Roeck, A. & Kado, M. The Higgs boson implications and prospects for future discoveries. *Nat. Rev. Phys.* **3**(9), 608-624 (2021).

 doi:10.20944/preprints202210.0172.v12

13. Weiss, L. S. et al. Controlled creation of a singular spinor vortex by circumventing the Dirac belt trick. *Nat. Commun.* **10**(1), 1-8 (2019).
14. Silagadze, Z. K. Mirror objects in the solar system?. *arXiv preprint astro-ph/0110161* (2001).
15. Rieflin, E. Some mechanisms related to Dirac's strings. *Am. J. Phys.* **47**(4), 379-380 (1979).
16. Yuguru, S. P. Unconventional reconciliation path for quantum mechanics and general relativity. *IET Quant. Comm.* **3**(2), 99–111 (2022).
17. Jaffe. R. L. Supplementary notes on Dirac notation, quantum states, etc. https://web.mit.edu/8.05/handouts/jaffe1.pdf (September, 2007).
18. Eigen, C. Spinors for beginners. https://www.youtube.com/@eigenchris (November, 2012)
19. Zhelobenko, D. P. Compact Lie groups and their representations. *J. Amer. Math. Soc.* **40**, 26-49 (1973).
20. https://en.wikipedia.org/wiki/Spinor (updated February 2024).
21. Burdman, G. Quantum field theory I_Lectures. http://fma.if.usp.br/~burdman (October, 2023).
22. Das, I. et al. *An introduction to physical chemistry*. New Age International (P) Limited, New Delhi, India (2005) 2nd Ed. pp 16-20.
23. Singh, R. B. *Introduction to modern physics*. New Age International (P) Limited, New Delhi, India (2009) 2nd Ed. Vol. 1, pp 420-425.